MITSUBISHI ELECTRIC RESEARCH LABORATORIES
http://www.merl.com

Consensus-based Synchronization of Microgrids at Multiple Points of Interconnection

Shah, S.; Sun, H.; Nikovski, D.N.; Zhang, J.

TR2018-112 August 17, 2018

Abstract

This paper presents a consensus-based distributed synchronization control method for microgrids with multiple points of interconnection. The proposed method can synchronize a microgrid at different points of interconnection using a common sparse communication network among its distributed generators. This functionality is critical for the networked operation of multiple microgrids in the future power systems. The proposed approach uses averaging and leader-follower modes of a commonly used consensus algorithm for multi-agent systems to achieve microgrid synchronization and smooth transition between the islanded and grid-connected modes at different interconnection points. The operation of the proposed distributed synchronization method is demonstrated on a microgrid with four inverters, each with an independent interconnection point to another microgrid or a bulk power system.

IEEE Power & Energy Society General Meeting

Consensus-based Synchronization of Microgrids at Multiple Points of Interconnection

Shahil Shah[1], Hongbo Sun[2], Daniel Nikovski[2], and Jinyun Zhang[2]

[1]Rensselaer Polytechnic Institute
Troy, NY 12180, USA
E-mail: shahs12@rpi.edu

[2] Mitsubishi Electric Research Laboratories
Cambridge, MA 02139, USA
Email: {hongbosun, nikovski, jzhang}@merl.com

***Abstract*–This paper presents a consensus-based distributed synchronization control method for microgrids with multiple points of interconnection. The proposed method can synchronize a microgrid at different points of interconnection using a common sparse communication network among its distributed generators. This functionality is critical for the networked operation of multiple microgrids in the future power systems. The proposed approach uses averaging and leader-follower modes of a commonly used consensus algorithm for multi-agent systems to achieve microgrid synchronization and smooth transition between the islanded and grid-connected modes at different interconnection points. The operation of the proposed distributed synchronization method is demonstrated on a microgrid with four inverters, each with an independent interconnection point to another microgrid or a bulk power system.**

Index Terms–**Synchronization, microgrid control, distributed generators, secondary control, distributed consensus control.**

I. Introduction

Microgrids are emerging as preferable solution for increasing the penetration of distributed energy resources in bulk power systems [1]. With the increasing number of microgrids, it will be important to be able to quickly and reliably connect them with each other or to a bulk power system whenever demanded by the transmission system operator. Because of wide geographical spread, it may be desired to connect multiple microgrids for improving reliability [2], which may result in multiple points of interconnection in a microgrid.

Synchronization parameters of a microgrid including voltage magnitude and frequency at a point of common coupling (PCC) depend on several distributed generators. Hence, the synchronization function is implemented at the centralized secondary level control, which achieves coordination among grid-forming generators in the microgrid [3]. When a microgrid is to be synchronized at a PCC, the difference between the frequency and voltage magnitudes of the microgrid and the power system are added to the centralized secondary control to eliminate the voltage and frequency errors. The phase synchronization is achieved either passively using a frequency offset or actively using a dedicated synchronizer [4].

The centralized nature of secondary control defies the fundamental objective of microgrids of providing an electrical and control infrastructure for the integration of distributed energy resources while keeping the central coordination at minimum. Two major disadvantages of centralized secondary control are existence of a single point-of-failure and requirement of communication from the secondary controller to each of the grid-forming generators in the microgrid. Additionally, centralized secondary control supports synchronization only at one point of interconnection. If there is an additional point of interconnection in the microgrid, additional secondary controller with remote sensing circuit is required at the new PCC if synchronization with a power system at the new PCC is desired. This will also require communication links from the new PCC to all the generators, leading to a dense communication network and low reliability.

Several distributed secondary control methods are proposed as alternative to centralized secondary control for voltage and frequency restoration after transients [5-7]. In these methods, each grid-forming generator has its own local secondary controller to eliminate the local frequency and voltage errors by vertically shifting its droop characteristics. A communication framework is also provided for coordinating the secondary controllers of generators to avoid disruption of power sharing among them. A simple and versatile distributed secondary control method is presented in [6, 7]. It requires each generator to communicate only with a few neighbor generators. It achieves the voltage and frequency restoration without disturbing power sharing through consensus among generators on the shifts of their droop characteristics. The consensus-based distributed secondary control method requires only a sparse communication network and it does not introduce a single-point-of-failure. However, the frequency and voltage references remain fixed in this method [7]. Hence, it is not applicable for synchronizing a microgrid with another power system, which requires the microgrid to track the frequency and voltage levels of the power system.

This paper builds upon the work in [7] and presents a distributed control method for synchronizing a microgrid with power systems located at different interconnection points using a common and sparse communication network among its grid-forming generators. The steady-state power sharing remains unaffected by the introduction of the distributed frequency and voltage synchronization control laws.

II. Consensus-Based Distributed Control

For a microgrid with n grid-forming generators, its communication network can be represented as a directed graph $G(V, \mathcal{E}, A)$ with node set $V = \{1,...,n\}$, edge set $\mathcal{E} \subseteq V \times V$, and adjacency matrix A [8]. If $(i, j) \in \mathcal{E}$, then there is a link directed from i^{th} to

j^{th} node, and the j^{th} node can receive information from the i^{th} node. Each link is associated with a positive weight $a_{ij} \in A$. A particular weight a_{ij} is zero, if there is no direct link between the i^{th} and j^{th} nodes. For an undirected graph $a_{ij} = a_{ji}$.

Two concepts of connectivity of graphs are important for this paper. First, an undirected graph is *connected* if there is an undirected path between any two distinct nodes. Second, in a directed graph G(V, $\mathcal{E}$, A), a graph $G_1(V_1, \mathcal{E}_1, A_1)$ is a *rooted directed spanning tree* if G_1 is a subgraph of the directed graph G(V, $\mathcal{E}$, A), it contains all the nodes of the parent directed graph G(V, $\mathcal{E}$, A), and it is a rooted directed tree. A rooted directed tree is a directed graph in which every node has exactly one parent except for the one, which has no parent and it is called root. In a rooted directed tree, a directed path exist from the root to all the other nodes in the tree.

Assume $x_i(t)$ represents an information state associated with i^{th} node. The most commonly applied algorithm for achieving consensus among the information states of nodes in a graph is [8]:

$$\dot{x}_i = -\sum_{j=1}^{n} a_{ij}(x_i - x_j) \text{ where } i \in V. \quad (1)$$

Two modes of the consensus algorithm are used in this paper:

1) Averaging Mode

For an undirected connected graph, the consensus algorithm results in the information states of all nodes to converge to a weighted average of their initial values [8]. If all non-zero weights a_{ij} are equal, the information states will converge to the average of their initial values. One trivial scenario is if the information states are at a common value when the consensus algorithm is activated, all the states will continue to stay at the same common value.

2) Leader-follower Mode

For a directed graph containing exactly one rooted directed spanning tree, the consensus algorithm in (1) results in information states of all the follower nodes to converge to the information state of the root node. The information state of the root node is independent of other nodes. For example, if k^{th} node is made the leader, its information state can follow an independent reference:

$$x_k = x_{ref} \quad (2)$$

III. Distributed Synchronization of Microgrids

A. Distributed Frequency Synchronization

The proposed method implements synchronization control based by adding a consensus-based synchronization layer to the distributed secondary control presented in [7]. The frequency droop control law including distributed synchronization and secondary control functions is:

$$\omega_i = (\omega^* + \Delta\omega_i^*) - m_i \cdot P_i + \Omega_i \quad (3)$$

where ω_i, m_i, and P_i are respectively the frequency, P-ω droop constant, and active power output of the i^{th} generator. ω^* is fixed nominal frequency reference.

Offset Ω_i and $\Delta\omega_i^*$ are outputs of respectively the distributed secondary control and the distributed synchronization control. Ω_i mitigates the error between the generator frequency ω_i and the frequency reference $(\omega^* + \Delta\omega_i^*)$. On the other hand, $\Delta\omega_i^*$ modifies the frequency reference of the i^{th} generator so that the generator frequency can track the frequency of the power system to which the microgrid is to be synchronized. The update laws for Ω_i and $\Delta\omega_i^*$ are discussed in the following.

The distributed secondary controller output Ω_i is updated based on the following consensus law:

$$k_i \frac{d\Omega_i}{dt} = -[\omega_i - (\omega^* + \Delta\omega_i^*)] - \sum_{j=1}^{n} a_{ij}(\Omega_i - \Omega_j) \quad (4)$$

The first part on the right-hand side of (4) ensures that the error between the generator frequency ω_i and modified frequency reference $(\omega^* + \Delta\omega_i^*)$ converges to zero in steady-state. The second part is similar to the consensus algorithm in (1) and it ensures that offsets Ω_i's of all the grid-forming generators are equal in steady-state. This preserves the active power sharing among generators depending on their droop slopes m_i's while achieving frequency regulation. The consensus among corrections Ω_i's only requires that the undirected graph formed by bidirectional communication links among grid-forming generators is connected. Hence, each generator does not require to communicate with all the remaining generators.

Frequency reference correction $\Delta\omega_i^*$ in (4) enables generator to track a time-varying frequency reference. $\Delta\omega_i^*$ at each generator is obtained according to the microgrid operation mode:

1) Leader-follower Mode

If the microgrid is to be synchronized at a point of interconnection near say k^{th} generator, the frequency reference correction at the k^{th} generator $\Delta\omega_k$ is obtained as difference between the measured frequency of the power system with which the microgrid is to be synchronized and the nominal reference ω^*:

$$\Delta\omega_k = \omega_{PCCk} - \omega^* \quad (5)$$

The frequency reference corrections at remaining generators are obtained using the following consensus law:

$$k_s \frac{d\Delta\omega_i}{dt} = -\sum_{j=1}^{n} a_{ij}(\Delta\omega_i - \Delta\omega_j) \text{ where } i \in V, i \neq k. \quad (6)$$

It can be inferred from (5) and (6) that the frequency reference correction states follow leader-follower mode described in Section II with generator k as the leader. Hence, the frequency references of all generators $(\omega^* + \Delta\omega_i)$ converge to the frequency of the power system at the k^{th} generator.

Fig. 1a) and c) respectively demonstrate synchronization at PCC-1 and PCC-2 using the proposed consensus-based method.

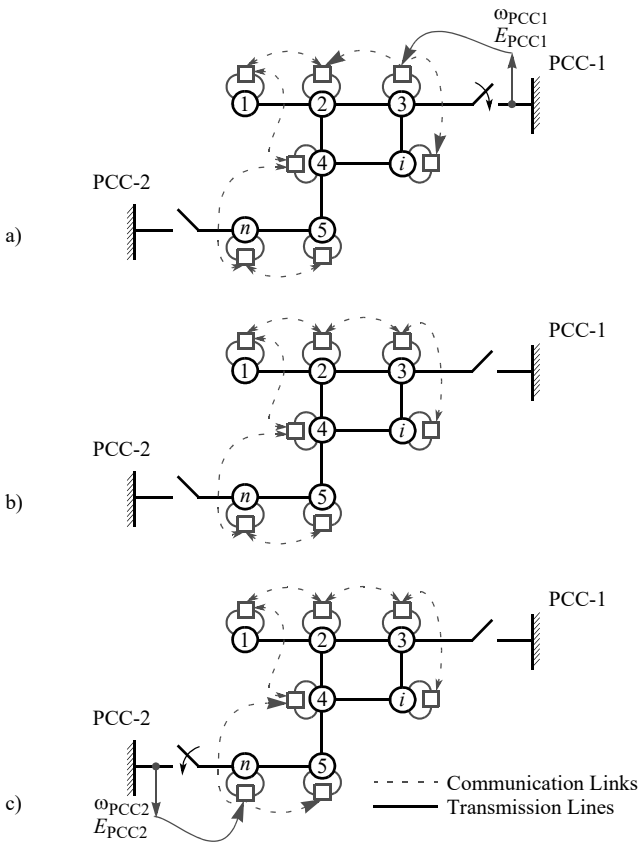

Fig. 1. Proposed distributed synchronization method. a) leader-follower mode for synchronization at PCC-1, b) averaging mode for islanded operation, and c) leader-follower mode for synchronization at PCC-2.

2) Averaging Mode

Once the microgrid is synchronized or if it has to return to the islanded mode, there is no need to keep one generator as the leader. Hence, the update law for the frequency reference correction states is switched to the averaging mode:

$$k_s \frac{d\Delta\omega_i}{dt} = -\sum_{j=1}^{n} a_{ij}(\Delta\omega_i - \Delta\omega_j) \text{ where } i \in \mathrm{V}. \qquad (7)$$

Fig. 1b) depicts the averaging mode of the distributed synchronization control. It is to be noted from Fig. 1 that the graph formed by communication links in the averaging mode is undirected and connected. Whereas, it becomes directed in the leader-follower mode as the links connected to the leader generator are modified from undirected bidirectional communication links to unidirectional links directed away from the leader.

B. Decoupling Consensus Algorithm and Frequency Control

In the leader-follower mode, all the frequency reference correction states $\Delta\omega_i$'s converge to the leader state $\Delta\omega_k$. They will continue to stay at the same value when the control is switched to the averaging mode. Hence, transition from the leader-follower mode to the averaging mode is smooth. However, transition from the averaging mode to the leader-follower mode is not smooth since the leader node will be the first to have information on the correction required in its frequency reference. The frequency reference correction states of the follower nodes will converge to that of the leader node with convergence rate depending on the speed of communication and the communication network topology [8]. It may happen that the leader generator starts changing its frequency toward that of the power system with which the microgrid is to be synchronized faster than the remaining generators can follow. This may transiently disturb active power sharing among generators and overload certain generators.

To avoid transient overloading, the frequency reference correction state at each generator, obtained using either (6) or (7), is passed through a low-pass filter before using it in (3) and (4). The output of the filter is indicated by an asterisk as $\Delta\omega_i^*$:

$$\frac{\Delta\omega_i^*}{\Delta\omega_i} = \frac{1}{1 + T_\omega \cdot s} \qquad (8)$$

Filter time-constant T_ω is kept few tens of times higher than the convergence rate of the consensus algorithm. This ensures that the frequency reference at each generator evolves at a rate much slower than the consensus algorithm used for distributed synchronization. This avoids large mismatch in the frequency references of generators and minimizes the transient overloading effect.

C. Distributed Voltage Synchronization

Distributed voltage synchronization is similarly achieved as frequency synchronization by introducing an information state in the *Q–V* droop control law representing correction to the nominal voltage reference *E**:

$$E_i = (E^* + \Delta E_i^*) - n_i \cdot Q_i + e_i \text{ where } i \in \mathrm{V} \qquad (9)$$

where E_i, n_i, and Q_i are respectively the voltage magnitude, *Q-V* droop constant, and reactive power output of the i^{th} generator. *E** is fixed nominal voltage reference.

Distributed synchronization control output ΔE_i^* modifies the voltage reference to track the voltage of the power system to which the microgrid is to be synchronized. Same as the distributed frequency synchronization, the voltage reference correction state ΔE_i^* is determined using either leader-follower mode or averaging mode. The consensus laws are similar to (6) and (7); they are not presented here because of space constraint. Same as frequency synchronization, the consensus algorithms for voltage synchronization and the voltage control of generators are decoupled using a low-pass filter with time constant T_E.

D. Interaction with Distributed Secondary Control

Distributed secondary control output e_i in (9) can be used to mitigate the error between the generator voltage E_i and reference $(E^* + \Delta E_i^*)$ while achieving reactive power sharing [6, 7]. However, because of the finite voltage drops across transmission lines, exact reactive power sharing cannot be achieved while regulating the voltages at generators at the same level [7]. This conflict can create potential stability problem in the distributed

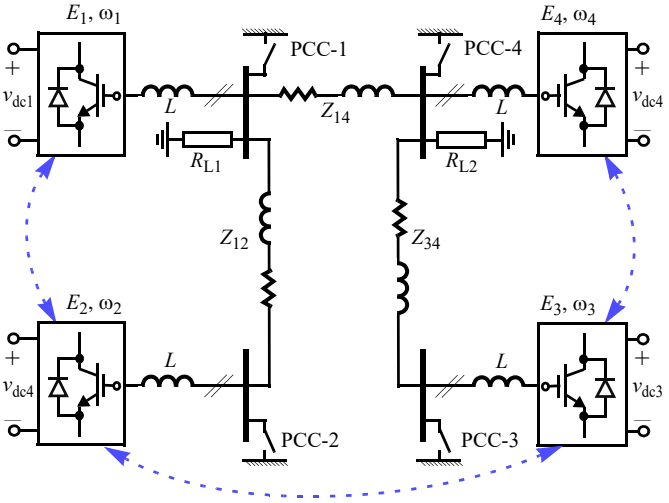

Fig. 2. Simulated microgrid. Dashed lines show communication links.

TABLE I PARAMETERS OF SIMULATED MICROGRID

Parameter	Value
Nominal grid voltage peak, E^*	325.3 V
Nominal frequency, ω^*	$2\pi\cdot 60$ rad/s
Phase reactor, L	1.8 mH
P-ω droop slopes: m_1 and m_4	$2.5\text{x}10^{-3}$
P-ω droop slopes: m_2 and m_3	$5.0\text{x}10^{-3}$
Transmission line impedance, Z_{12}	$0.8 + j3.6\text{x}10^{-3}$
Transmission line impedance, Z_{14}	$0.4 + j1.8\text{x}10^{-3}$
Transmission line impedance, Z_{34}	$0.7 + j1.9\text{x}10^{-3}$
Distributed secondary control gain, k_i	2.0
Communication network weights, a_{ij}	a_{12}, a_{21}, a_{23}, a_{32}, a_{34}, a_{43} are unity; Other weights are zero
Distributed synchronization gain, k_s	0.2
Low-pass filter time-constant, T_ω, T_E	10

secondary voltage control [7]. Possible interaction between the proposed distributed voltage synchronization and distributed secondary voltage control may further deteriorate the microgrid stability and must be properly investigated. Such analysis is beyond the scope of this paper; the reactive power sharing is not considered in the following by dropping the terms on the right-hand side of (9) that are outside of the parenthesis.

IV. SIMULATION CASE STUDY

The operation of the proposed distributed synchronization method is demonstrated by a simulation case study of single-phase microgrid shown in Fig. 2 [7]. It has four voltage-controlled voltage source inverters acting as grid-forming generators and two loads R_{L1} and R_{L2}, connected respectively at the inverter-1 and inverter-4. The microgrid has four different PCCs that can be used to connect it with adjacent power grids. Parameters of the simulated microgrid are shown in Table I. Each inverter in the microgrid implements the P–ω droop control law in (3) to develop its frequency reference ω_i. Since the reactive power sharing is not considered, the voltage reference of each inverter is set to $(E^* + \Delta E_i^*)$.

Fig. 3 and 4 show simulated responses of the islanded microgrid in Fig. 2. Fig. 3 shows frequencies, voltage magnitudes, and calculated active power outputs of all the four inverters. Fig. 4 shows information states including Ω_i (distributed secondary control), $\Delta\omega_i$ (distributed frequency synchronization), and ΔE_i (distributed voltage synchronization) at all the four inverters.

Events during the simulation period are described below:

- t_0: Simulation is started with the distributed synchronization control in the averaging mode,
- t_1: Distributed synchronization control is changed to the leader-follower mode with inverter-1 as the leader. Its information states $\Delta\omega_1$ is reduced from 0 to $-2\pi\cdot 1$ rad/s to reduce the microgrid frequency from 60 to 59 Hz, and ΔE_1 is increased to $0.05\cdot E^*$ to increase the microgrid voltage by 5% above the nominal voltage E^*.
- t_2: Inverter-3 is made the leader. Its frequency correction state $\Delta\omega_3$ is kept equal $-2\pi\cdot 1$ and the voltage correction state ΔE_3 is reduced to $-0.05\cdot E^*$ to reduce the microgrid voltage by 5% below the nominal voltage E^*.
- t_3: Inverter-4 is made the leader. Its frequency correction state $\Delta\omega_4$ is increased to $2\pi\cdot 1$ to increase the microgrid frequency to 61 Hz and the voltage correction state ΔE_4 is made equal to $-0.02\cdot E^*$ to increase the microgrid voltage to 2% below the nominal voltage E^*.
- t_4: Load R_{L2} is doubled from 2 kW to 4 kW.

After the simulation is started at t_0, the distributed secondary control information states Ω_i's start increasing to restore the microgrid frequency to 60 Hz. The total load on the microgrid is 4 kW, which is shared by the four inverters depending on the P–ω droop slopes m_i's. Active power supplied by inverters 1 and 4 is double than that supplied by inverters 2 and 3 because the droop slopes m_1 and m_4 are half than the droop slopes m_2 and m_3. The distributed synchronization states in Fig. 4b) and c) continue to stay at a common value because of the averaging mode.

Inverter-1 is assigned the leader at t_1 and the distributed synchronization control is changed from the averaging mode to the leader-follower mode. The distributed synchronization information states of the remaining inverters start approaching that of the inverter-1, as seen in Fig. 4b) and c). Since, the follower inverters take sometime before converging their synchronization information states to that of the inverter-1, there is a transient power mismatch among the inverters, as seen in Fig. 3c). The transient power mismatch is minimized by using a low-pass filter as discussed in Section III B. Depending on the synchronization information states set by the leader inverter-1, the microgrid frequency and voltage settle respectively to 59 Hz and $1.05\cdot E^*$. Distributed synchronization is switched back to the averaging mode at around 30s without resulting in any transients.

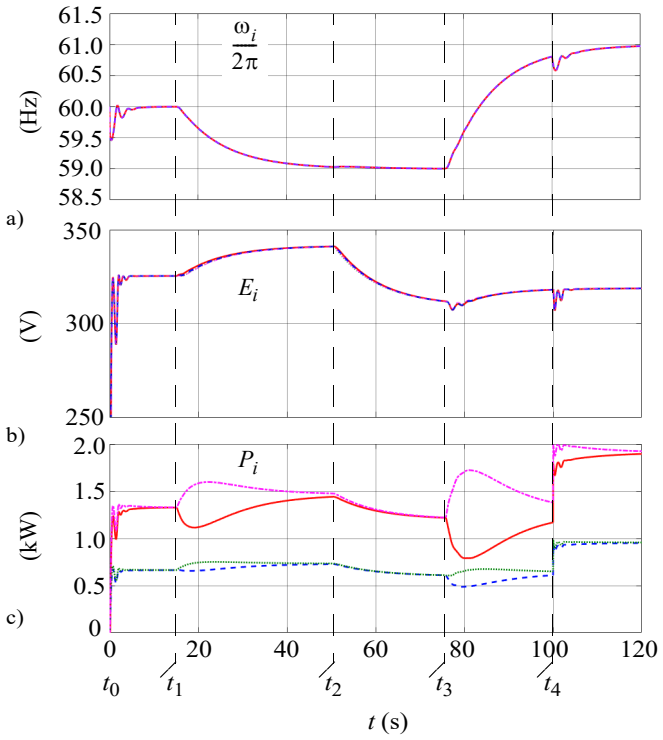

Fig. 3. Performance of distributed synchronization control: a) Inverter output voltage frequencies $\omega_i/(2\pi)$, b) inverter output voltage magnitudes E_i, and c) inverter active power outputs P_i. Solid red lines: inverter-1, dashed blue lines: inverter-2, dotted green lines: inverter-3, and dashed-dotted pink lines: inverter-4.

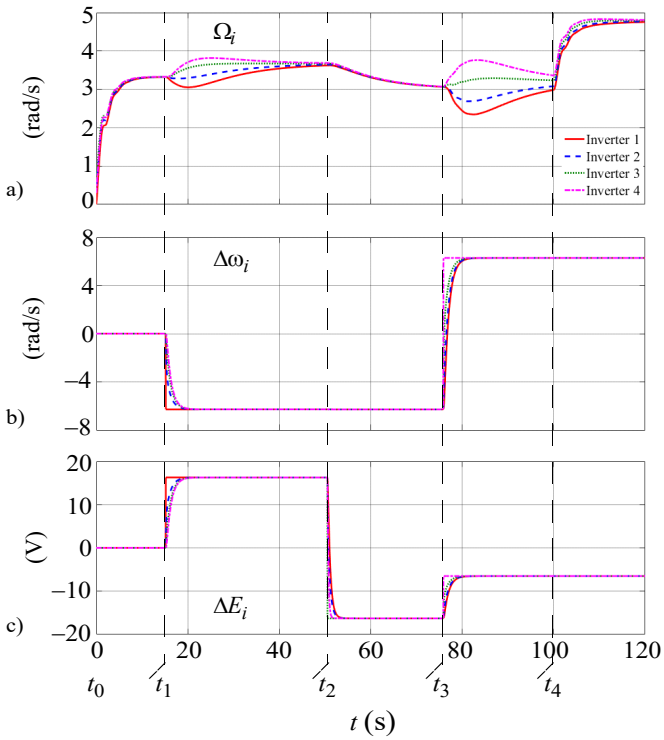

Fig. 4. Information states of distributed secondary and distributed synchronization control. a) Secondary frequency control output Ω_i, b) distributed frequency synchronization control output $\Delta\omega_i$, and c) distributed voltage synchronization control output ΔE_i. Solid red lines: inverter-1, dashed blue lines: inverter-2, dotted green lines: inverter-3, and dashed-dotted pink lines: inverter-4.

At t_2, the inverter-3 is made the leader. Since the inverter-3 does not demand change in the microgrid frequency, there is no disturbance in the active power sharing among the inverters at t_2. The microgrid voltage settles to a new value $0.95{\cdot}E^*$ depending on ΔE_3 set by the inverter-3.

At t3, the inverter-4 is made the leader and it is evident from Fig. 3 and 4 that the microgrid frequency and voltage converge to values demanded by the leader inverter-4.

At t_4, load R_{L2} is increased from 2 to 4 kW, making the total load on the microgrid to be 6 kW. It is to be noted that the synchronization states in Fig. 4b) and c) remain unaffected as the load transients are unrelated to the distributed synchronization dynamics. On the other hand, the distributed secondary control information states Ω_i's start increasing to compensate for the increment in the total microgrid load and restore the frequency back to the value demanded by the leader inverter.

V. Conclusion

This paper proposed a consensus-based distributed synchronization method for microgrids with multiple points of interconnection. Unlike centralized secondary control based synchronization approach, the proposed method does not require separate communication system for each interconnection point and it enables microgrid synchronization at multiple interconnection points using a common sparse communication network. Future work will investigate the effects of the proposed distributed synchronization method on the reactive power sharing performance and the stability of the microgrid.

References

[1] *Microgrid Controllers – The Heart and Soul of Microgrid Automation*, *IEEE Power Energy Mag.*, vol. 15, no. 4, July/Aug. 2017.

[2] M. Shahidehpour, Z. Li, S. Bahramirad, Z. Li, and W. Tian, "Networked microgrids" *IEEE Power Energy Mag.*, vol. 15, no. 4, pp.63-71, July/Aug. 2017.

[3] J. M. Guerrero, J. C. Vasquez, J. Matas, L. G. de Vicuna, and M. Castilla, "Hierarchical control of droop-controlled ac and dc microgrids – a general approach toward standardization," *IEEE Trans. Ind. Electron.*, vol. 58, no. 1, pp. 158-172, Jan. 2011.

[4] S. Shah, H. Sun, D. Nikovski, and J. Zhang, "VSC-based active synchronizer for generators," *IEEE Trans. Energy Conv.*, Early Access, 2017.

[5] Q. Shafiee, J. M. Guerrero, and J. C. Vasquez, "Distributed secondary control for islanded microgrids—a novel approach," *IEEE Trans. Power Electron.*, vol. 29, no. 2, pp. 1018-1031, Feb. 2014.

[6] J. W. Simpson-Porco, F. Dorfler, and F. Bullo, "Synchronization and power sharing for droop-controlled inverters in islanded microgrids," *Automatica*, vol. 49, no. 9, pp. 2603-2611, Sep. 2013.

[7] J. W. Simpson-Porco, Q. Shafiee, F. Dorfler, J. C. Vasquez, J. M. Guerrero, and F. Bullo, "Secondary frequency and voltage control of islanded microgrids via distributed averaging," *IEEE Trans. Ind. Electron.*, vol. 62, no. 11, pp. 7025-7038, Nov. 2015.

[8] W. I. Ren, R. W. Beard, E. M. Atkins, "Information consensus in multivehicle cooperative control," *IEEE Control Syst. Mag.*, vol. 27, no. 2, pp. 71-82, April 2007.